Spatiotemporal Distribution of *b* Value Estimated from Seismic Activity in the Northern Part of Tokushima Prefecture: A Report as of April 2024 in Tokushima City and Surrounding Municipalities

Toshiki SHIMBARU [1*]

1 Information Processing Center, Seinan Gakuin University
6-2-92 Nishijin, Sawara-ku, Fukuoka-shi, Fukuoka 814-8511 Japan
E-mail: shimbaru@seinan-gu.ac.jp
* Corresponding Author

Abstract

In recent studies, several cases have been reported in which the *b* value decreased in the vicinity of the mainshock location before a major earthquake. Therefore, the *b* value, which represents the characteristics of seismic activity in each region, is attracting attention because it may provide helpful information for identifying locations where large earthquakes are likely to occur in the future. The authors have observed the spatial distribution of *b* values in shallow inland areas of Japan and have continued investigating areas with low *b* values. This study focused on the northern part of Tokushima Prefecture and observed the spatial distribution of the latest *b* values from seismic activity up to April 1, 2024. As a result, a low *b* value area was observed at a depth of around 10 km in Tokushima City and its surrounding cities. The results of the ΔAIC test showed no significant temporal change in the *b* value in this region, but the most recent *b* value was as low as 0.63. Depending on the magnitude of future earthquakes, it is possible that a significant decrease in the *b* value could be observed. Therefore, it is necessary to continue to monitor future seismic activity closely.

Keywords

b value, Spatiotemporal distribution, Seismic activity, Kamiura-Nishitsukinomiya fault, Northern part of Tokushima Prefecture, Tokushima City

1. Introduction

The Gutenberg-Richter law (G-R law) (Gutenberg and Richter 1944) is an empirical rule for the frequency distribution of earthquakes of different magnitudes in a given space-time. This empirical law is expressed by the following equation (1), using the magnitude *M* (magnitude of earthquake) and the total number *N*(*M*) of earthquakes of that magnitude or larger. The *b* value, the coefficient of *M* in equation (1), is usually around 0.7 to 1.1 (Utsu 2001). In the time-space, where the frequency of large earthquakes is relatively high, the *b* value is small.

$$\log_{10} N(M) = a - bM \quad (1)$$

Previous studies (Nanjo *et al*. 2012, Nanjo *et al*. 2016, Shimbaru and Yoshida 2021) have reported that a decrease in the *b* value was observed near the locations that later became epicenters of large earthquakes. These findings suggest that the *b* value might help identify the locations of future large earthquakes. Consequently, there have been attempts to use real-time monitoring of the spatiotemporal distribution of *b* values to predict large earthquakes (Gulia and Wiemer 2019, Nanjo 2020). The authors have observed the spatial distribution of *b* values in Japan's shallow inland areas and investigated regions with low *b* values, such as the northwestern part of the Kego fault (Shimbaru 2023). This report describes the actual situation as of April 1, 2024, in the low *b* value region observed near Tokushima City in the northern part of Tokushima Prefecture.

2. Seismic activity in the research area

Fig. 1 shows the area covered by this study. Fig. 1(a) shows the epicentral distribution of earthquakes of *M* 0 or greater that occurred at shallow depths of 0~20 km during 1997/10/01~2024/03/31, and Fig. 1(b) shows the seismic activity trends. These earthquakes' location, magnitude, and occurrence time were obtained from the Japan Meteorological Agency's earthquake catalog. No notable seismic activity has occurred within Fig. 1(a). However, further back in the past, an earthquake of *M* 5.6 (maximum intensity 4) occurred on 1947/01/16. In Fig. 1 (a), part of the Median Tectonic Line active fault zone extends to the north. According to the government's long-term assessment (The Headquarters for Earthquake Research Promotion 2017a), an earthquake of about *M* 7.7 is possible in this section. In addition, the Kamiura-Nishitsukinomiya fault is known in the south. The magnitude of earthquakes expected on this fault is about *M* 6.5 (The Headquarters for Earthquake Research Promotion 2017b). Fig. 1(c) shows the magnitude-frequency distribution of earthquakes within Fig. 1(a). From this figure, the author determined that *M* 0.5 is the minimum size at which all earthquakes were detected without omission and decided to use earthquakes above *M* 0.5 to estimate the *b* value.

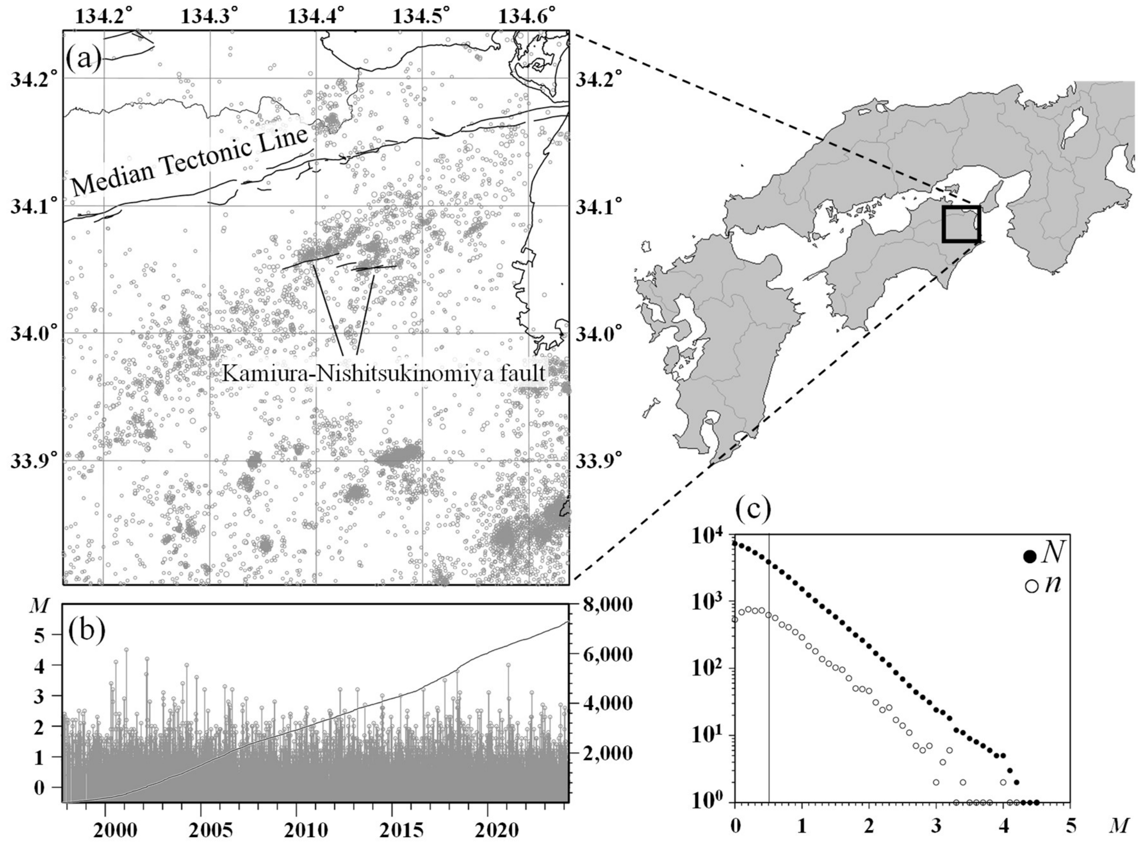

Fig. 1. (a) Epicentral distribution of earthquakes during 1997/10/01~2024/03/31 ($M \geq 0$, depth ≤ 20 km). Solid lines indicate active faults. (b) Magnitude-Time (*M-T*) diagram with the cumulative number of earthquakes of $M \geq 0$ in the area. (c) Frequency-magnitude distribution of earthquakes in the study area. The white and black circles represent incremental and cumulative frequencies, respectively. All earthquakes with $M \geq 0.5$ are considered to be detected throughout the period.

3. Methods

The method of drawing the spatial distribution of *b* values in this report is based on Shimbaru (2021). First, grid points were placed at 0.5-minute intervals (approximately 1 km) in the latitude and longitude directions and at 1 km intervals in the depth direction. A spherical space with a radius of 4 km was set up for each grid point. The dataset consists of the last 200 earthquakes that occurred within this space. If 200 earthquakes could not be secured by going back to 1997/10/01, the number was assumed to be up to that time. Next, for each dataset, M_c (Magnitude of completeness) was estimated as the minimum magnitude of the earthquake that could be detected without omission. The specific method for estimating M_c followed Wiemer and Wyss (2000). That is, assuming that the magnitude-frequency distribution of earthquakes follows the G-R law, and M_c was set as the smallest size satisfying a goodness of fit (*R* value) of 90 % or more with the ideal distribution. Once this M_c is estimated, the *b* value can be obtained from the following equation (2a) by the maximum likelihood method (Utsu 1965). In this equation, $\bar{M}$ represents the mean of the magnitudes of earthquakes greater than or equal to M_c in the dataset. However, since M is graded in units of ΔM (=0.1), the actual calculation must use equation (2b) to consider this bias (Marzocchi and Sandri 2003).

$$b = \log_{10} e \,/(\bar{M} - M_c) \quad (2a)$$
$$b = \log_{10} e \,/\{\bar{M} - (M_c - \Delta M/2)\} \quad (2b)$$

In this process, if the R value did not meet 90 % or the number of earthquakes above M_c was fewer than 50, the obtained b value was considered unreliable and unknown. The estimation error σ of the b value obtained from N earthquakes over M_c was calculated using equation (3) (Shi and Bolt 1982).

$$\sigma = 2.30 \times b^2 \times \sqrt{\sum_{i=1}^{N}(M_i - \bar{M})^2 \,/N(N-1)} \quad (3)$$

When displaying the spatial distribution of three-dimensional b values as a plan view, the smallest value among the b values at different depths at the same place was displayed since this report aims to detect locations with low b values.

4. Results and Discussion

Fig. 2(a) shows the spatial distribution of b values in the study area in April 2014 and April 2024 and the change in b values (Δb) at each time point during the period concerning April 2014. The depth at which the b value was adopted is shown in Fig. 2(b), and the M_c estimated along with the b value is shown in Fig. 2(c). The A-B cross section in Fig. 2(a) is overlaid on the distribution of seismic activity around the Kamiura-Nishitsukinomiya fault, and the dip is vertical. The spatial distribution of b values on the A-B cross section is shown in Fig. 2(d). In this figure, the grid points are located at intervals of 1 km each in the horizontal and depth directions on the A-B section. The b value is calculated using earthquakes within a space of a radius of 4 km from each grid point, with unknown locations in gray. In locations with few earthquakes, the dataset dates back to October 1997, and the number of earthquakes used to estimate the b value is often only 100 or so grid points. Furthermore, there are fewer than 50 earthquakes above M_c on the surrounding grids, and b values are unknown for many of the grids. In Fig. 2(a), region 1 was set to enclose the area where the b value is lower than the surrounding area. Within region 1, the b value appears to decrease gradually throughout the period. Fig. 2(b) and 2(d) show that the b value is lowest around 10 km depth. During this time, M_c in Fig. 2(c) hardly changes from 0.5, and the b value is obtained stably. As an example, Fig. 2(e) shows the magnitude-frequency distribution of earthquakes used to calculate the b value at a grid point (point e in Fig. 2(a)) in region 1 as of April 1, 2024. It shows that the minimum M_c is estimated within a range that does not deviate from the theoretical G-R law.

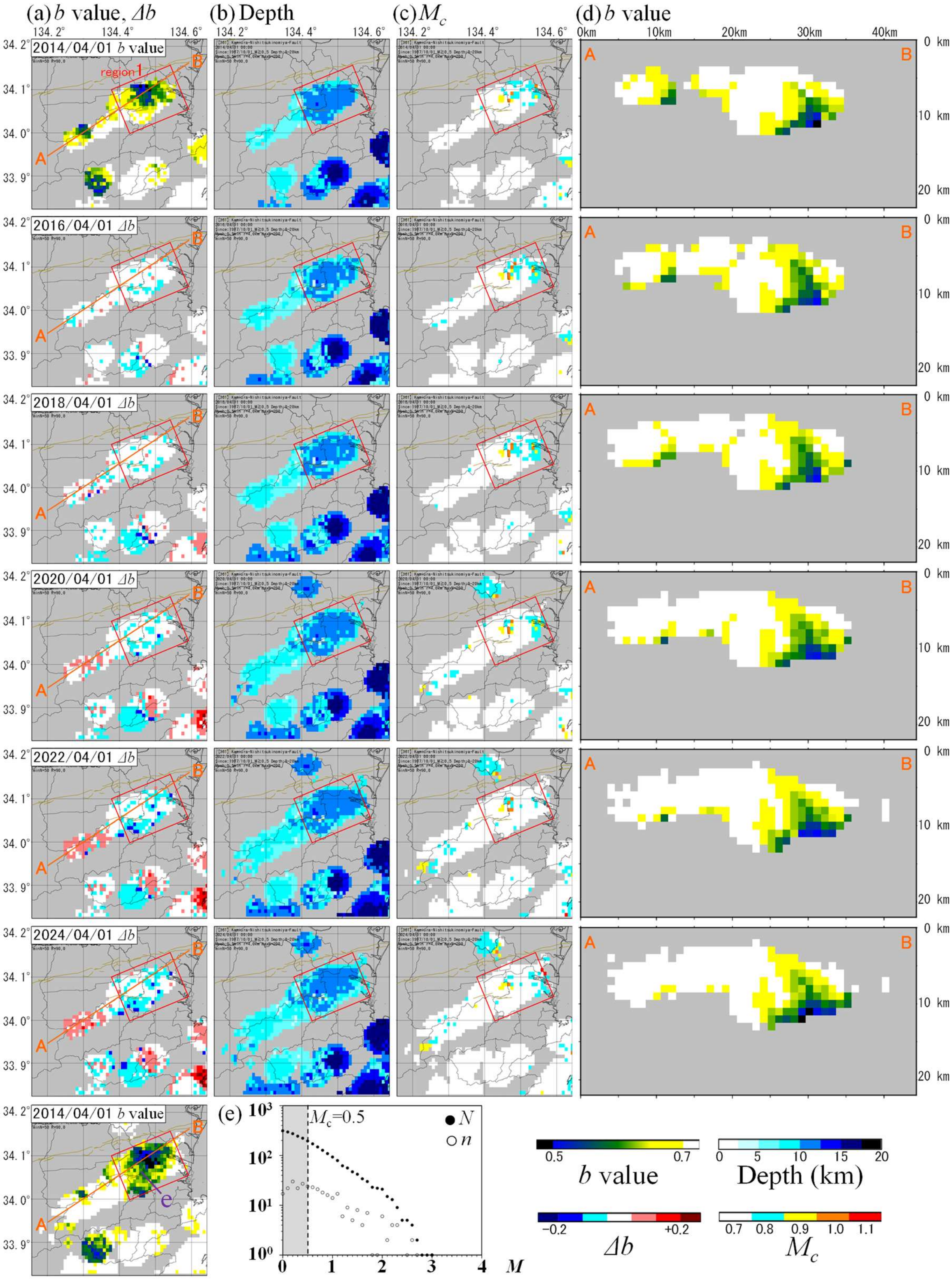

Fig. 2. (a) Spatial distribution of *b* value from April 2014 to April 2024. The middle figures show *Δb* from April 2014. (b) The depth of the grid points from which the *b* value was obtained. (c) M_c estimated together with the *b* value. (d) Spatial distribution of *b* value on the A-B plane. (e) Example of the frequency-magnitude distribution of earthquakes used to calculate the *b* value for a grid point.

Next, the time variation of the *b* value was determined using earthquakes that occurred at depths of 0~20 km in region 1. Fig. 3 shows the evolution of seismic activity within this region and the results of repeated calculations of *b* values, sliding the data set of 200 earthquakes by 40. The horizontal lines extending from each point in Fig. 3 indicate the duration of the earthquake dataset, and the vertical lines indicate the estimation error σ. Table 1 shows the *b* values and M_c obtained from the data sets for each period indicated by (1) to (10) in Fig. 3. M_c is 0.5 in all cases from (2) to (10), and the *b* value is generally obtained stably. To determine the significance of the time variation of the *b* value, ΔAIC was calculated from the following equation (4) according to Utsu (1999). Each variable in equation (4) represents the number of earthquakes in the two datasets to be compared (N_1 and N_2) and the *b* values obtained from each dataset (b_1 and b_2). If ΔAIC is greater than 2, the difference in *b* values is considered significant.

$$\Delta AIC = -2(N_1 + N_2)\ln(N_1 + N_2) + 2N_1 \ln\left(N_1 + N_2\frac{b_1}{b_2}\right) + 2N_2 \ln\left(N_1\frac{b_2}{b_1} + N_2\right) - 2 \quad (4)$$

A comparison between periods (5) and (10), in which the data sets did not overlap, revealed a ΔAIC of 1.04, with no significant change identified between the two periods. However, the *b* value obtained from the most recent activity is low at 0.63, and a significant decrease in the *b* value may be observed depending on the magnitude of future earthquakes.

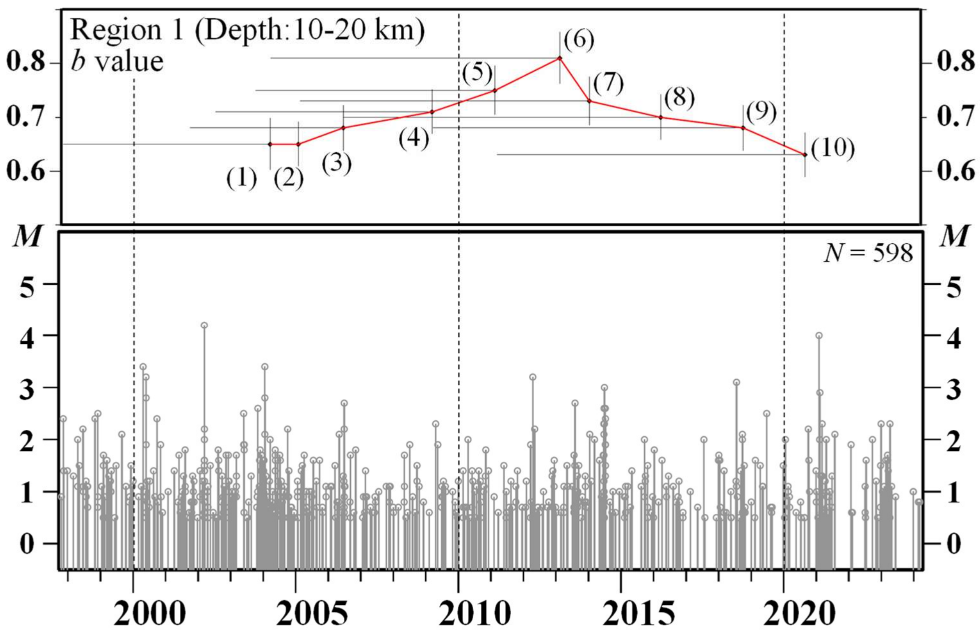

Fig. 3. Temporal variation of *b* value (upper panel) and Magnitude-Time (*M-T*) diagram (lower panel) in region 1. Each *b* value was obtained using 200 datasets. The Summary of *b* values indicated by the (1) ~ (10) symbols is listed in Table 1.

Table 1. A summary of the *b* values obtained for each period in Fig. 3.

Dataset Period		*b* value	M_c	*ΔAIC*
(1)	1997/10/21 ~ 2004/05/16	0.65	0.7	—
(2)	2000/01/03 ~ 2005/04/07	0.65	0.5	—
(3)	2001/11/01 ~ 2006/09/08	0.68	0.5	—
(4)	2002/08/22 ~ 2009/06/30	0.71	0.5	—
(5)	2003/11/29 ~ 2011/07/01	0.75	0.5	—
(6)	2004/05/19 ~ 2013/07/22	0.81	0.5	—
(7)	2005/04/28 ~ 2014/06/30	0.73	0.5	—
(8)	2006/09/09 ~ 2016/10/02	0.70	0.5	—
(9)	2009/07/11 ~ 2019/05/13	0.68	0.5	—
(10)	2011/07/27 ~ 2021/04/29	0.63	0.5	1.04 (5)→(10)

5. Conclusion

This report focuses on the northern part of Tokushima Prefecture and observes the spatial distribution of the latest *b* values from seismic activity up to April 1, 2024, and confirms a low *b* value area at depths of around 10 km, mainly in Tokushima City and its surrounding cities. The results of the *ΔAIC* test showed no significant temporal change in the *b* value in this region, but the most recent *b* value was as low as 0.63. Depending on the magnitude of future earthquakes, it is possible that a significant decrease in the *b* value could be observed. Therefore, it is necessary to continue to monitor future seismic activity closely.

Acknowledgment

This report uses the Japan Meteorological Agency's earthquake catalog with permission based on data provided by the following institutions: National Research Institute for Earth Science and Disaster Resilience, Hokkaido University, Hirosaki University, Tohoku University, the University of Tokyo, Nagoya University, Kyoto University, Kochi University, Kyushu University, Kagoshima University, National Institute of Advanced Industrial Science and Technology (AIST), Geospatial Information Authority of Japan (GSI), Japan Agency for Marine-Earth Science and Technology (JAMSTEC), Association for the Development of Earthquake Prediction, Aomori Prefecture, Tokyo Metropolitan Government, Shizuoka Prefecture, Hot Springs Research Institute of Kanagawa Prefecture, and Japan Meteorological Agency. Some figures were created using the epicenter display program (Yokoyama 1997) and GMT (Wessel and Smith 1998).

References

Gulia L, Wiemer S (2019) Real-time discrimination of earthquake foreshocks and aftershocks. Nature 574:193-199. https://doi.org/10.1038/s41586-019-1606-4

Gutenberg B, Richter CF (1944) Frequency of earthquakes in California. Bulletin of the Seismological Society of America 34(4):185-188. https://doi.org/10.1785/BSSA0340040185

Marzocchi W, Sandri L (2003) A review and new insights on the estimation of the *b*-value and its uncertainty. Annals of Geophysics 46(6):1271-1282. https://doi.org/10.4401/ag-3472

Nanjo KZ, Hirata N, Obara K, Kasahara K (2012) Decade-scale decrease in *b* value prior to the M9-class 2011 Tohoku and 2004 Sumatra quakes. Geophysical Research Letters 39(20):L20304. https://doi.org/10.1029/2012GL052997

Nanjo KZ, Izutsu J, Orihara Y, Furuse N, Togo S, Nitta H, Okada T, Tanaka R, Kamogawa M, Nagao T (2016) Seismicity prior to the 2016 Kumamoto earthquakes. Earth Planets Space 68:187. https://doi.org/10.1186/s40623-016-0558-2

Nanjo KZ (2020) Were changes in stress state responsible for the 2019 Ridgecrest, California, earthquakes?. Nature Communications 11:3082. https://doi.org/10.1038/s41467-020-16867-5

Shi Y, Bolt BA (1982) The standard error of the magnitude-frequency *b* value. Bulletin of the Seismological Society of America 72(5):1677-1687. https://doi.org/10.1785/BSSA0720051677

Shimbaru T, Yoshida A (2021) The *b* value in the seismic activity around foci of large crustal earthquakes before and after their occurrence. Zisin (Journal of the Seismological Society of Japan. 2nd ser.) 74:77-86. https://doi.org/10.4294/zisin.2020-5

Shimbaru T (2023) Recent spatial distribution of *b* value around the northwestern part of the Kego fault. Zisin (Journal of the Seismological Society of Japan. 2nd ser.) 76:1-6. https://doi.org/10.4294/zisin.2022-9

The Headquarters for Earthquake Research Promotion (2017a) Long-term Evaluation of the Median Tectonic Line active fault zone (Kongosanchitoen-Yufuin) (Version 2). https://www.jishin.go.jp/main/chousa/katsudansou_pdf/20171219_mtl.pdf. Accessed 11 Apr 2024

The Headquarters for Earthquake Research Promotion (2017b) Long-term Evaluation of the Kamiura-Nishitsukinomiya fault. https://www.jishin.go.jp/main/chousa/17dec_chi_shikoku/shikoku_04_kamiura-nishitsukinomiya.pdf. Accessed 11 Apr 2024

Utsu T (1965) Method for determining the value of *b* in a formula log $n=a-bM$ showing the magnitude-frequency relation for earthquakes. Geophysical bulletin of the Hokkaido University 13:99-103. https://doi.org/10.14943/gbhu.13.99

Utsu T (1999) Representation and analysis of the earthquake size distribution: A historical review and some new approaches, Pure and Applied Geophysics 155:509-535. https://doi.org/10.1007/s000240050276

Utsu T (2001) Distribution of magnitude of earthquakes. Utsu T (ed) Seismology, 3rd ed. K YORITSU SHUPPAN CO., LTD., Tokyo

Wessel P, Smith WHF (1998) New, improved version of generic mapping tools released. EOS Trans. AGU 79(47):579. https://doi.org/10.1029/98EO00426

Wiemer S, Wyss M (2000) Minimum magnitude of completeness in earthquake catalogs: Examples from Alaska, the Western United States, and Japan. Bulletin of the Seismological Society of America 90(4):859-869. https://doi.org/10.1785/0119990114